E1-2022-29

V. I. Yurevich *

PHENOMENOLOGICAL MODEL
OF NUCLEON-INDUCED FISSION CROSS SECTIONS
IN HIGH-ENERGY REGION

* E-mail: yurevich@jinr.ru

Юревич В. И.   E1-2022-29

Феноменологическая модель сечений деления,
вызванного нуклонами высоких энергий

Разработана феноменологическая модель для аппроксимации и численной оценки сечений деления при взаимодействии нуклонов высоких энергий с тяжелыми ядрами. Предсказания модели сравниваются с наиболее надежными экспериментальными данными, имеющимися оценками и теоретическими расчетами для различных ядер от ^{181}Ta до ^{239}Pu. Модель хорошо воспроизводит экспериментальные результаты выше 50 МэВ и обладает хорошим предсказательным потенциалом.

Yurevich V. I.   E1-2022-29

Phenomenological Model of Nucleon-Induced Fission
Cross Sections in High-Energy Region

A phenomenological model was developed for approximation and numerical estimation of fission cross sections in interactions of high-energy nucleons with heavy nuclei. The model predictions are compared with the most reliable experimental data, available estimations and theoretical calculations for different nuclei from ^{181}Ta to ^{239}Pu. The model reproduces well the experimental results above 50 MeV and has good prediction potential.

INTRODUCTION

The decay of the excited nuclear system produced in the interaction of high-energy nucleons with heavy nuclei has a multi-step character which is a challenge for both theoretical description and experimental study. There is a great number of papers dedicated to this phenomenon with the study of different aspects of the nuclear system evolution. The fission reaction is one of the decay processes, the probability of which depends on the characteristics of fissile nucleus and its excitation energy, which is a function of the type and energy of incident nucleons.

Up-to-date nuclear technologies based on the application of accelerators need precise data on fission cross sections. Another need for these data is the development of theoretical codes for the description of high-energy nucleon–nucleus interactions. These needs initiate the activity for experimental study of the fission reaction at high energies and data evaluation [1–3]. Another way is the development of theoretical models and codes for the calculation of fission cross sections [4–12] or the development of expressions based on approximation formulas [13–15] and phenomenological models [16] reproducing available experimental results. Nowadays, the theoretical approach can be used only for rough estimation since the models are under development and need precise experimental data for studying the model validation. The prediction potential of the approximation formulas is based on the set of experimental data used, but in the high-energy region it is rather poor, and it leads to high uncertainty in the fission cross section predictions. Thus, the development of a phenomenological model, the expression of which has a physical interpretation, might give a good tool for the description of the nucleon-induced fission cross sections in the high-energy region. In this paper, a novel phenomenological model developed for this aim is discussed.

1. FISSION IN HIGH-ENERGY REGION

With an increase in energy in the region above ~ 50 MeV, the mechanism of interaction of nucleons with heavy nuclei completely changes from the production and decay of an excited compound nucleus to an intra-nuclear cascade.

In the region of hundreds of MeV, the fission probability of the residual nucleus is characterized by the competition of two processes. With an increase in the excitation energy, the probability of the fission increases. But the

1

process of fast emission of particles with some loss of mass and charge of the residual nucleus decreases the parameter of fissility. The same situation takes place for peripheral collisions at higher energies. This phenomenon is called a spallation reaction.

In central collisions at energies above ~ 600 MeV, a new process of energy transfer occurs by the excitation of baryon resonances and the meson production. The excitation energy reaches several MeV per nucleon [17–22], and as a result, the residual nuclear system becomes unstable to further expansion under the action of thermal energy and the Coulomb forces. In about 100 fm/c (freeze-out time), the system decays into free nucleons and nuclear fragments, a multifragmentation process. The composition of nuclear fragments depends on the excitation energy, and it can be a combination of nucleons, light charged particles (LCPs) and massive residue or, at high excitation, with multiple production of intermediate mass fragments (IMFs). The fast decay of high-excited nuclear system suppresses the decay by fission mode, and the fission becomes a peripheral process in this energy region.

The reaction picture described above is supported by experimental results on the mass distribution of residual nuclei and its dependence on the incident nucleon energy [23–28]. If the energy range is below 200 MeV, a peak of fission fragments is observed in the middle of the scale. It has a good separation from a narrow peak of nuclei with masses close to the mass of the target nucleus. With an increase in energy to several GeV, the mass distribution covers the entire interval from the mass of hydrogen isotopes up to the target nucleus mass.

There are a large number of experiments dedicated to the study of the evolution and decay of an excited nuclear system produced in high-energy reactions. The obtained results on the secondary particle and nuclei distributions and the production cross sections show a weak dependence of these values on the projectile energy in the region above 10 GeV. It proves the hypothesis of limiting fragmentation and predicts similar behavior for inelastic, fragmentation and fission cross sections.

The described picture of fission in high-energy nucleon–nucleus interactions is the basis of the phenomenological model discussed below.

2. PHENOMENOLOGICAL MODEL

The developed model is based on the assumption that the fission cross section σ_f of the target nucleus with charge and mass numbers Z_T and A_T may be written as a superposition of two terms — the fissility of the excited residual nucleus produced after the fast phase of nucleon–nucleus interaction P_f and the inelastic cross section σ_{in} reduced by subtracting the contribution of other decay processes, spallation, fragmentation and multifragmentation, which are faster than fission. The sum cross section of these processes is marked as σ_{fr}. Then the expression for the fission cross section is

$$\sigma_f = P_f(\sigma_{\text{in}} - \sigma_{\text{fr}}). \tag{1}$$

2

All the terms of this expression are written as a superposition of two functions. The first function depends on the characteristics of the target nucleus Z_T and A_T, and the second one reproduces the dependence on the kinetic energy of incident nucleon. Also, by taking into account the well known phenomenon of limiting fragmentation in the energy range above 10 GeV, it is suggested that the energy dependence of all the terms of this expression becomes small with energy and the functions describing the energy dependences tend to unit. As a result, the expression (1) may be presented as

$$\sigma_f = \sigma_{\text{in}}(A_T) P_f(x) F_f(E)[F_{\text{in}}(E) - k(A_T) F_{\text{fr}}(E)]. \tag{2}$$

The function of fissility of the residual nucleus is described with the formula

$$P_f(x) = \exp\left[C(x - B)\right], \tag{3}$$

where

$$x \equiv x_R = x_T + \delta = Z_T^2/A_T + \delta \tag{4}$$

is an effective fissility parameter of the residual nucleus after the first fast phase of interaction calculated as the sum of the fissility parameter of the target nucleus and the correction term δ obtained by fitting to experimental data. The values of the parameters C and B were chosen as 0.62 and 37.9, respectively.

The inelastic cross section is described with the expressions proposed by Letaw et al. [29] for interactions of protons with nuclei:

$$\sigma_{\text{in}} = \sigma_{\text{in}}(A_T) F_{\text{in}}(E), \tag{5}$$

$$\sigma_{\text{in}}(A_T) = 45 A_T^{0.7}[1 + 0.016 \sin(5.3 - 2.63 \ln A_T)], \tag{6}$$

$$F_{\text{in}}(E) = 1 - 0.62 \exp\left(-\frac{E}{200}\right) \sin(10.9 E^{-0.28}), \tag{7}$$

where E is the kinetic energy of incident proton in MeV.

Here, these expressions are used for both types of projectiles because of the small deviation between the values of the inelastic cross section predicted for pA and nA reactions and the poor data set for neutron-induced reactions in the high-energy region. The calculated magnitudes have a maximum uncertainty in the energy interval below 200 MeV. It has to be noted that in this region a deviation of more than 10% between approximations proposed by different authors is also observed.

The functions $F_f(E)$ and $F_{\text{fr}}(E)$ have a threshold character, and they are described with the following expression:

$$F(E) = \begin{cases} \exp[-(a/(E/E_{\text{th}} - 1))^\alpha], & E > E_{\text{th}} \\ 0, & E \leqslant E_{\text{th}} \end{cases}, \tag{8}$$

where the parameters a, α and effective threshold energy E_{th} are obtained by fitting to the selected reliable experimental data.

3

The obtained magnitudes of parameters of the function $F_f(E)$ are given in Table 1. For the (p, f) reaction with pre-actinide nuclei, the obtained values for the parameters E_{th} and a are well described by the formulas

$$E_{\text{th}} = 2577 - 153.6\, x_T + 2.329\, x_T^2, \tag{9}$$

$$a = 385.8 - 18.85\, x_T + 0.218\, x_T^2. \tag{10}$$

The parameter α is a constant (see Table 1). For actinide nuclei, there is a small variation of the parameter values, and some of them do not depend on the type of target nucleus.

For all fission reactions, the parameter values of the function $F_{\text{fr}}(E)$ were used as $a = 10$, $\alpha = 1$ and $E_{\text{th}} = A_T$ (MeV). This means that the processes of spallation and fragmentation begin to make their contribution to inelastic cross section in the energy region where the excitation energy exceeds ~ 1 MeV/nucleon.

Table 1. The parameters of the function $F_f(E)$ obtained by fitting to the experimental data

Reaction	Nucleus	E_{th}, MeV	a	α
Pre-actinides				
(n, f)	^{209}Bi	10	27	0.8
(p, f)	^{181}Ta	73	19.72	0.47
	^{197}Au	48	7.40	0.47
	^{208}Pb	44.5	4.02	0.47
	^{209}Bi	44	1.27	0.47
Actinides				
(n, f)	^{232}Th	3.5	6	1.2
	^{238}U	3.5	2.86	1.2
	^{235}U	3.5	1.49	1.2
	^{237}Np	2.0	2.6	1.2
	^{239}Pu	2.0	2.6	1.2
(p, f)	^{232}Th	8	1.5	1.2
	^{238}U	8	1.25	1.2
	^{235}U	8	1.25	1.2
	^{237}Np	8	1.25	1.2
	^{239}Pu	8	1.25	1.2

For example, the functions $F_{\text{in}}(E)$, $F_f(E)$ and $F_{\text{fr}}(E)$ for the fission cross sections of two nuclides ^{238}U and ^{209}Bi are shown in Fig. 1.

The term $k(A_T)$ is the ratio of the cross sections:

$$k(A_T) = \sigma_{\text{fr}}(A_T)/\sigma_{\text{in}}(A_T) \approx \sigma_{\text{geom}}^{\text{core}}/\sigma_{\text{geom}}, \tag{11}$$
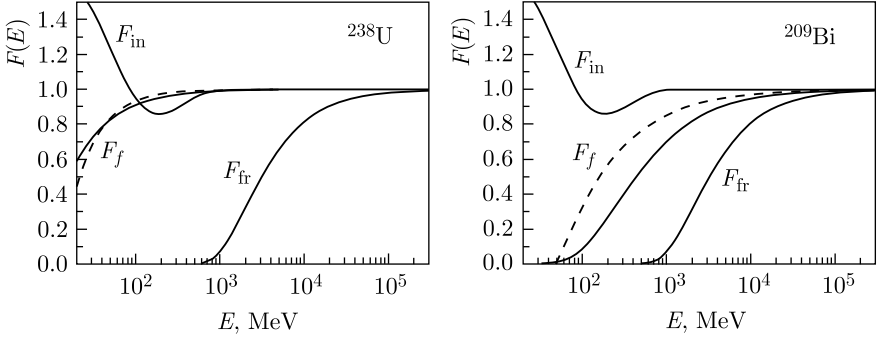
which varies from 0.47 for Ta to 0.5 for actinide nuclei.

Fig. 1. Functions $F_{\text{in}}(E)$, $F_f(E)$ and $F_{\text{fr}}(E)$ obtained for ^{238}U (left) and ^{209}Bi (right). Two functions F_f shown as solid and dashed curves correspond to (n, f) and (p, f) reactions, respectively

The fitting to the experimental data for (n, f) and (p, f) cross sections gave a small difference between the values of the effective fissility parameters of the residual nuclei x_R^p and x_R^n. This leads to a decrease in the dependence of the fission cross section on the type of incident nucleon with energy.

The deviation of x_R from x_T is shown in Fig. 2 as a function of the fissility parameter of the target nucleus $x_T = Z_T^2/A_T$ together with the approximation curve described by the formula

$$x_R - x_T = \begin{cases} 24.72 - 1.246\,x_T + 0.0168\,x_T^2, & x_T < 35.56 \\ 30.67 - 0.809\,x_T, & x_T \geqslant 35.56 \end{cases} \tag{12}$$

The shown dependence of the deviation leads us to the conclusion that with a decrease in the fissility parameter of the target nucleus x_T, the fission of residual nuclei requires an increase in the effective number of emitted neutrons during the fast phase of reaction.
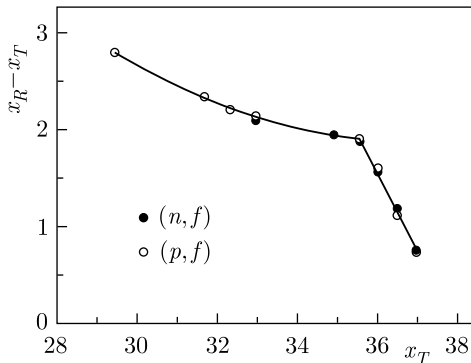

Fig. 2. The deviation of the effective fissility parameter of the residual nuclei x_R from the fissility parameter of the target nucleus x_T as a function of x_T

3. NEUTRON-INDUCED FISSION CROSS SECTIONS

The available set of experimental data on fission cross sections for high-energy nucleon–nucleus interactions is very limited and especially above the energy of 1 GeV. The most reliable data on neutron-induced fission cross sections are recent evaluation for ^{209}Bi(n, f), ^{235}U(n, f), ^{238}U(n, f) and ^{239}Pu(n, f) proposed as neutron standards in the energy range up to 200 MeV [1]. Also, the first three reactions were recommended as reference data in the energy interval from 200 to 1000 MeV [2]. For the ^{232}Th(n, f) reaction, the model prediction is compared with the data [30] and the result of the n_TOF collaboration [31] in the energy ranges up to 400 and 1000 MeV, respectively. Over the last 20 years, the main efforts have
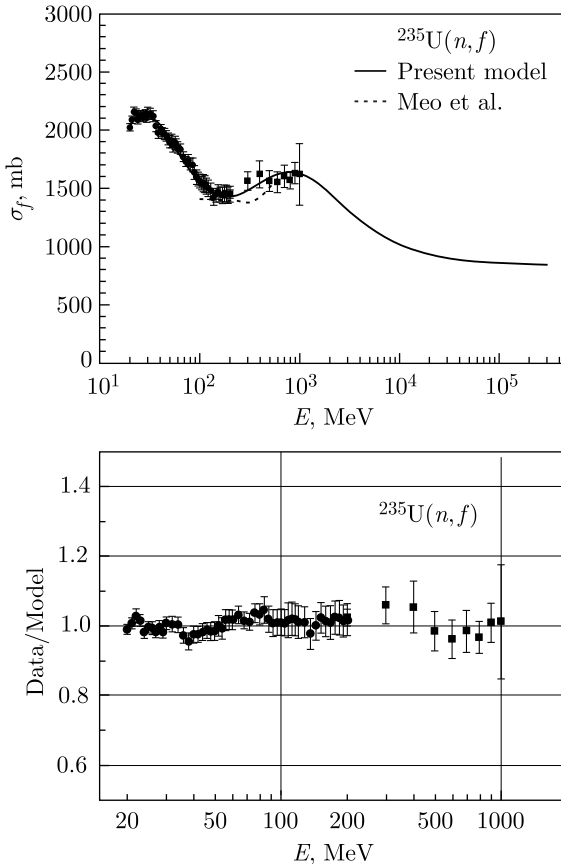
Fig. 3. The neutron-induced fission cross section of ^{235}U (top) and the ratio of the recommended data (points) [1, 2] to magnitudes calculated with the model expression (bottom)

been undertaken by the n_TOF collaboration at CERN, and its experimental program continues [31–33].

First of all, the model has to describe the evaluated data on neutron-induced fission cross sections of ^{235,238}U and ^{209}Bi [1, 2] in the energy range up to 1000 MeV. The comparison of experimental data with the calculated values is shown in Figs. 3–5 for these nuclei, respectively.

The comparison shows that the model expression reproduces well the data above 20 MeV for ^{235}U(n, f) and ^{238}U(n, f), and above 50 MeV for ^{209}Bi(n, f). The shown ratios clearly prove that the deviations do not exceed $\sim 5\%$.

For ^{232}Th(n, f) below 1 GeV, the model prediction shown in Fig. 6 does not contradict the experimental data obtained by Lisowski et al. [30] and the n_TOF collaboration [31], and it agrees with the theoretical calculation [11].
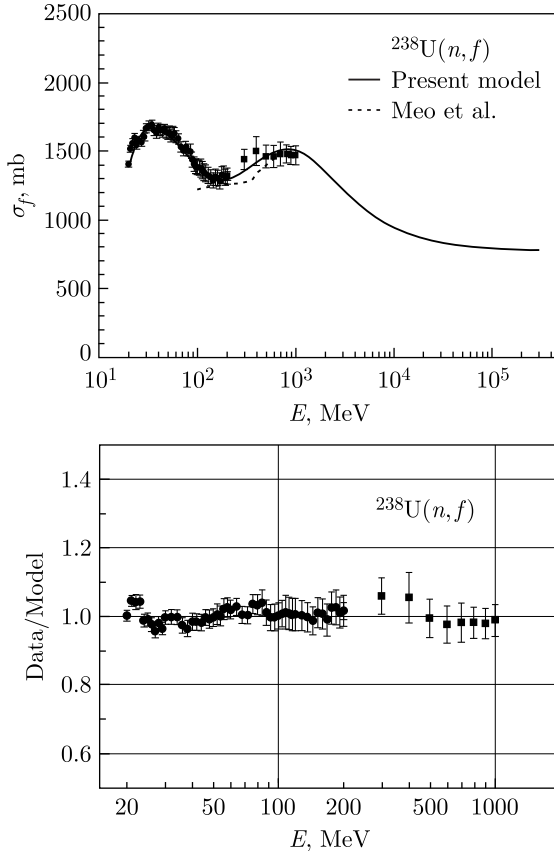

Fig. 4. The neutron-induced fission cross section of ^{238}U (top) and the ratio of the recommended data (points) [1, 2] to magnitudes calculated with the model expression (bottom)
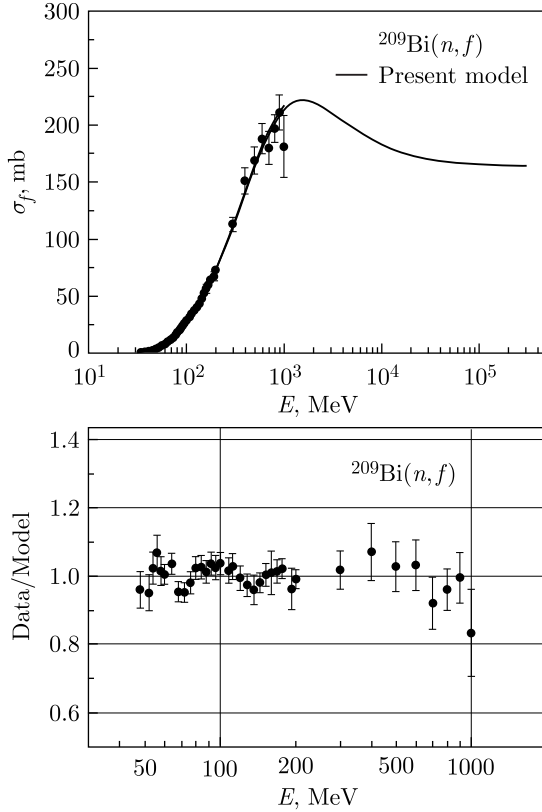
7

Fig. 5. The neutron-induced fission cross section of ^{209}Bi (top) and the ratio of the recommended data (points) [1, 2] to magnitudes calculated with the model expression (bottom)
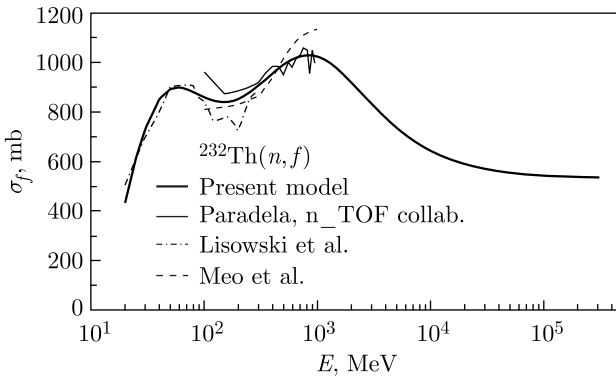

Fig. 6. The neutron-induced fission cross sections of ^{232}Th

The model curve for ^{237}Np(n, f) shown in Fig. 7 has a small deviation from the results of the n_TOF collaboration [32] below 300 MeV. But at higher energies, the model predicts a slight increase in the cross section in contradiction with the n_TOF data following down with energy.

The evaluated data for ^{239}Pu(n, f) [1] are in good agreement with the model curve, as is shown in Fig. 8.
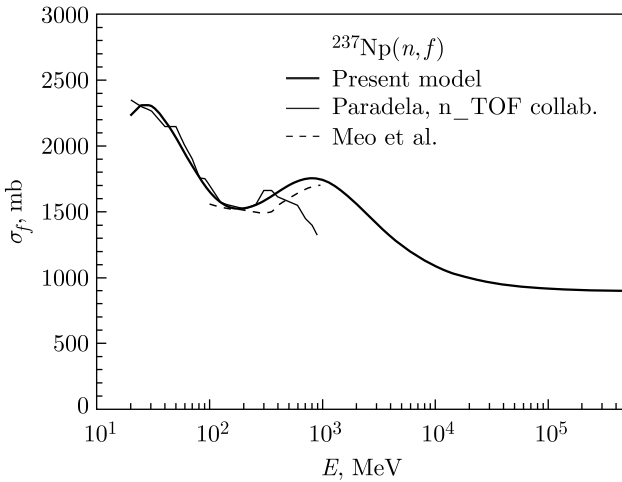

Fig. 7. The neutron-induced fission cross sections of ^{237}Np
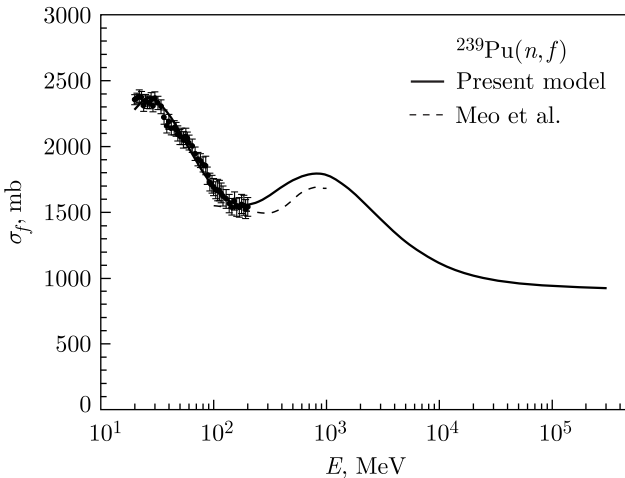

Fig. 8. The neutron-induced fission cross sections of ^{239}Pu. The symbols are the experimental data

4. PROTON-INDUCED FISSION CROSS SECTIONS

The approbation of the model for the description of proton-induced fission cross sections was fulfilled using the results of recent measurements at PNPI for a wide set of nuclei in the energy range from 200 to 1000 MeV [34, 35] together with data of other groups [36–53]. Additionally, the model was compared with the data file JENDL/HE [3] at energies below 200 MeV and with Prokofiev approximation [13] that used experimental results obtained before 2001.

The model description of the PNPI results [34, 35] obtained for various pre-actinide nuclei and three isotopes of uranium is shown in Fig. 9. As one can see, the model curves fit well the experimental points for all target nuclei.
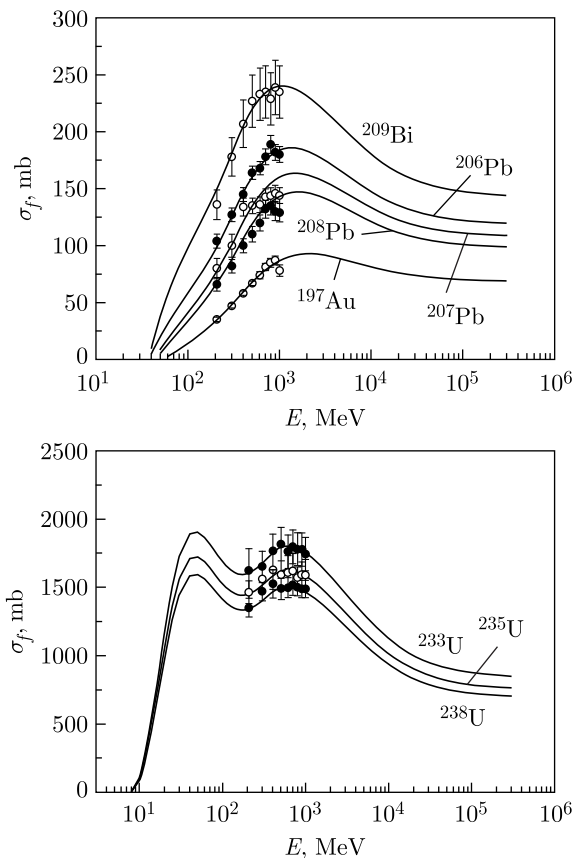

Fig. 9. The proton-induced fission cross sections of ^{197}Au, ^{206,207,208}Pb, ^{209}Bi (top) and ^{233,235,238}U (bottom). The points — the experimental data [34, 35], the curves — the present model

The proton-induced fission cross sections for ^{238}U and ^{209}Bi are shown in Fig. 10. Here the model curves are compared with the experimental data, the JENDL/HE data file [3] in the energy region below 200 MeV, the Prokofiev approximation [13], and the prediction of theoretical model of Meo et al. [11] in the energy range from 100 to 1000 MeV. A good agreement between the model curves and the experimental results is observed. At low energies, the model satisfactorily agrees with the JENDL/HE data file, and it is not in contradiction with the theoretical calculations [11]. But it is important to note that there is an essential disagreement between the model and the Prokofiev approximation.

The proton-induced fission cross sections of nuclei lighter than bismuth, ^{208}Pb and ^{197}Au, are shown in Fig. 11. In the energy range below 1 GeV, the model curve for ^{208}Pb(p, f) agrees well with the JENDL/HE data file [3] and
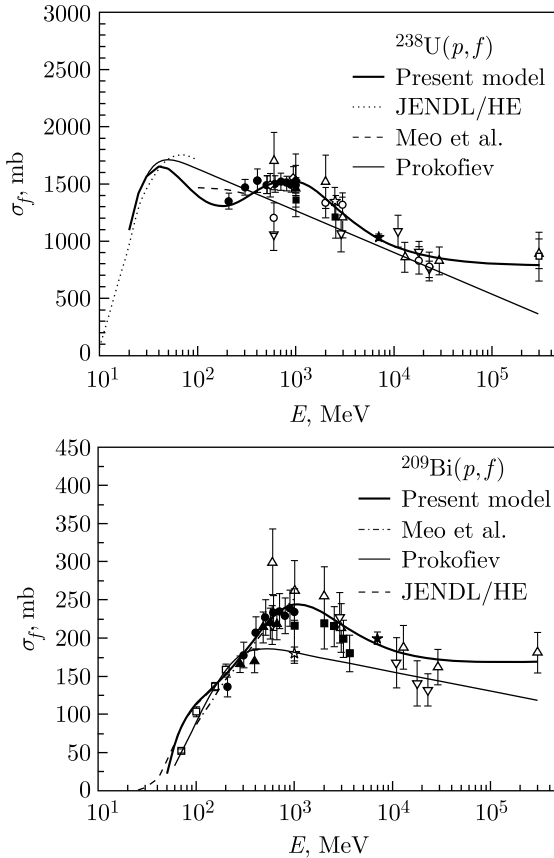

Fig. 10. The proton-induced fission cross sections of ^{238}U (top) and ^{209}Bi (bottom). The symbols are the experimental data
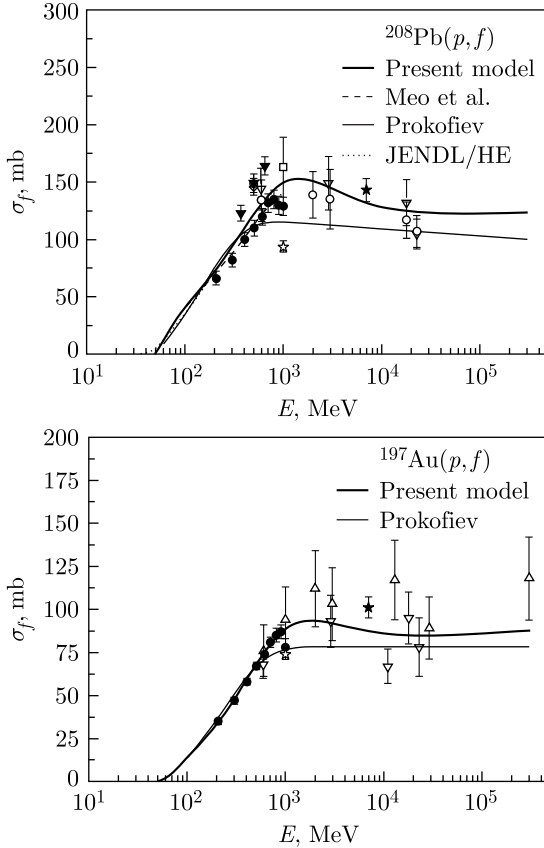
Fig. 11. The proton-induced fission cross sections of ^{208}Pb (top) and ^{197}Au (bottom). The symbols are the experimental data

the theoretical model [11]. But the curve lies between the PNPI data [34] and the results obtained in GSI [42, 47]. The results of GSI are essentially larger than the PNPI data, and this difference has to be understood. A possible reason may be connected with methodical errors since the measurement in PNPI is a fixed target experiment, and the GSI data were obtained in reverse kinematics. The predicted energy dependence of the fission cross section of ^{197}Au follows the PNPI data [35] up to 1 GeV. For both reactions, the model predictions are in good agreement with the Prokofiev approximation [13] below 400 MeV and with available experimental data above 1 GeV.

The comparison of the (p, f) cross sections predicted by the developed model and the Prokofiev approximation [13], which does not include experimental results obtained over the last 20 years, shows an underestimation of the cross section values by the approximation formula in the energy range above ~ 400 MeV.

5. DISCUSSION OF THE RESULTS

The study of the developed model performance demonstrates a good potential of the model for the prediction of (n, f) and (p, f) cross sections for actinides in the energy range above 50 MeV.

The energy region below 1 GeV is complicated for the description of the energy dependence of the fission cross sections due to specifics of the nucleon–nucleus interaction in this energy region. The main sources of prediction errors are the uncertainties of the used inelastic cross section formula [29] and the parameters of the function P_f, which are not independent of each other.

Above 1 GeV, the energy dependence of the fission cross sections is defined by the function $f_{\mathrm{fr}}(E)$ and the parameter k, which describe the contribution of fast decay processes in competition with fission. And in the range above 10 GeV, the fission cross sections have a slight dependence on the energy of incident nucleons tending to constant values.

The proton-induced fission cross sections of actinides shown in Fig. 12 (left) have two wide peaks: one peak at 40–50 MeV and the other around 800 MeV. The pre-actinides have one peak similar to the second one for actinides, but it tends to disappear from bismuth to tantalum with a simultaneous decrease in the fission cross section magnitude, as is shown in Fig. 12 (right).

The comparison of (n, f) and (p, f) cross sections shows a trend to close values with increasing energy. A large difference is observed for actinides only below 50 MeV, where $\sigma(n, f)$ exceeds $\sigma(p, f)$. For pre-actinides, a discrepancy between these values is observed in the energy region below a few GeV, where incident protons induce fission with higher cross section than neutrons with the same energy. Two examples, the fission cross sections of ^{238}U and ^{209}Bi, are shown in Fig. 13. It is clearly seen that for ^{238}U in the range above
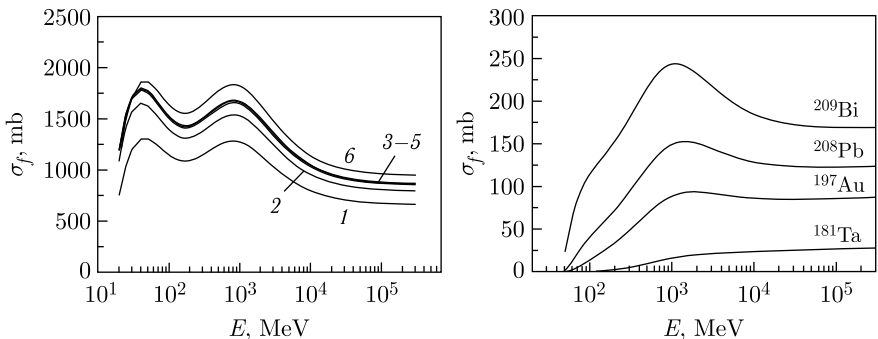

Fig. 12. The proton-induced fission cross sections of actinides (left: 1 — ^{232}Th; 2 — ^{238}U; 3–5 — ^{235}U, ^{337}Np, ^{239}Pu; 6 — ^{233}U) and pre-actinides (right) obtained with the model expression
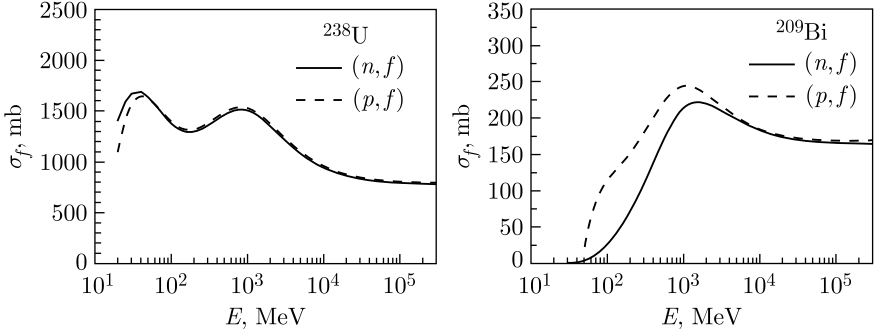
Fig. 13. The comparison of (n, f) and (p, f) cross sections of ^{238}U (left) and ^{209}Bi (right) calculated with the model expression

the first peak, the difference between $\sigma(n, f)$ and $\sigma(p, f)$ is rather small. For bismuth, it comes only above energy of ~ 2.5 GeV.

As the functions $F_{\mathrm{in}}(E)$, $F_f(E)$ and $F_{\mathrm{fr}}(E)$ tend to unit with energy above 10 GeV, the fission cross sections in this energy range tend to limit values in accordance with the model expression (2):

$$\sigma_f^{\mathrm{HE}} = \sigma_{\mathrm{in}}(A_T)P_f(x)[1 - k(A_T)]. \tag{13}$$

The magnitudes of σ_f^{HE} together with the values of x_R, σ_{in}, P_f and k used in calculation with this expression are given in Table 2 for different heavy nuclei.

T a b l e 2. The fission cross sections in very high energy region σ_f^{HE} and the values of x_R, σ_{in}, P_f and k for different heavy nuclei

Target nucleus	x_T	x_R	σ_{in}, mb	P_f	k	σ_f^{HE}, mb
^{181}Ta	29.44	32.24	1689	0.0299	0.47	26.77
^{197}Au	31.68	34.02	1795	0.0902	0.48	84.19
^{208}Pb	32.33	34.53	1875	0.1238	0.483	120.0
^{209}Bi	32.96	35.07	1875	0.1762	0.483	170.8
^{232}Th	34.91	37.0	2025	0.5904	0.5	597.8
^{238}U	35.56	37.45	2063	0.7565	0.5	780.3
^{235}U	36.02	37.58	2044	0.8303	0.5	848.6
^{237}Np	36.49	37.68	2057	0.8725	0.5	897.4
^{239}Pu	36.97	37.71	2070	0.8872	0.5	918.3

The following formula gives a good fit to the values σ_f^{HE}:

$$\sigma_f^{\mathrm{HE}} = \begin{cases} -185208 + 180445\, x_T - 586.4\, x_T^2 + 6.358\, x_T^3 & \text{for Au−Th} \\ -106191 + 5803\, x_T - 78.61\, x_T^2 & \text{for Th−Pu} \end{cases}. \tag{14}$$
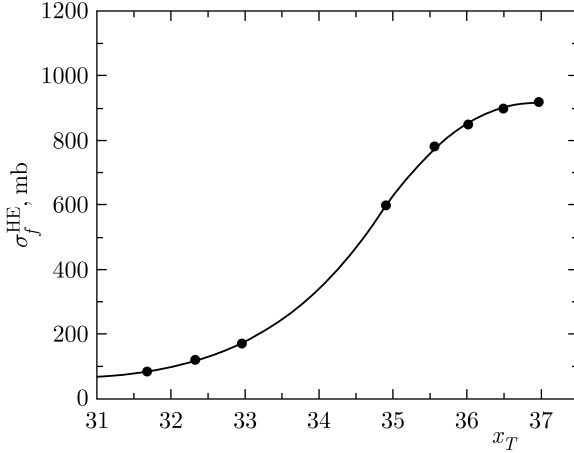
14

Fig. 14. The fission cross sections σ_f^{HE} in the very high energy range from Au to Pu. The points — the calculation with expression (13), the curve — the approximation (14)

This approximation, together with the magnitudes of σ_f^{HE} given in Table 2, is shown in Fig. 14. It is clearly seen that the effective fissility parameter of residual nuclei is always larger than the same parameter of a target nucleus. This is the result of nucleon emission (mainly neutrons) during the fast phase of the reaction that precedes the fission. The difference grows with decreasing x_T of a target nucleus. For example, one may conclude that the effective number of emitted neutrons before fission of ^{181}Ta exceeds the neutron loss in fission of ^{239}Pu with a difference of about 10 neutrons.

A comparison of the recent theoretical calculations [10, 12] of the fission cross sections ^{238}U(p, f), ^{197}Au(p, f) and ^{181}Ta(p, f) in the energy range up to 8 GeV with the prediction of the phenomenological model and experimental
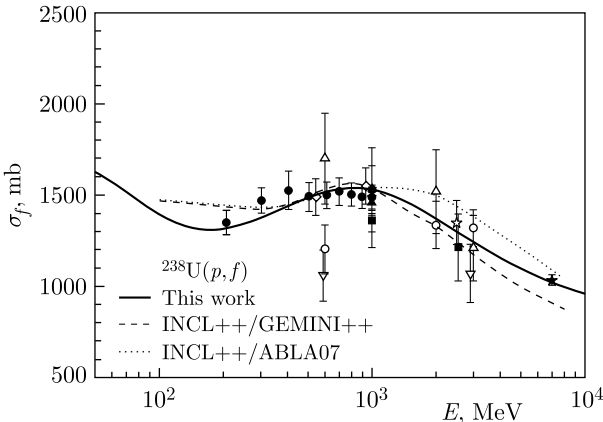

Fig. 15. The comparison of the model prediction of fission cross section ^{238}U(p, f) with the theoretical calculations [12] and experimental data
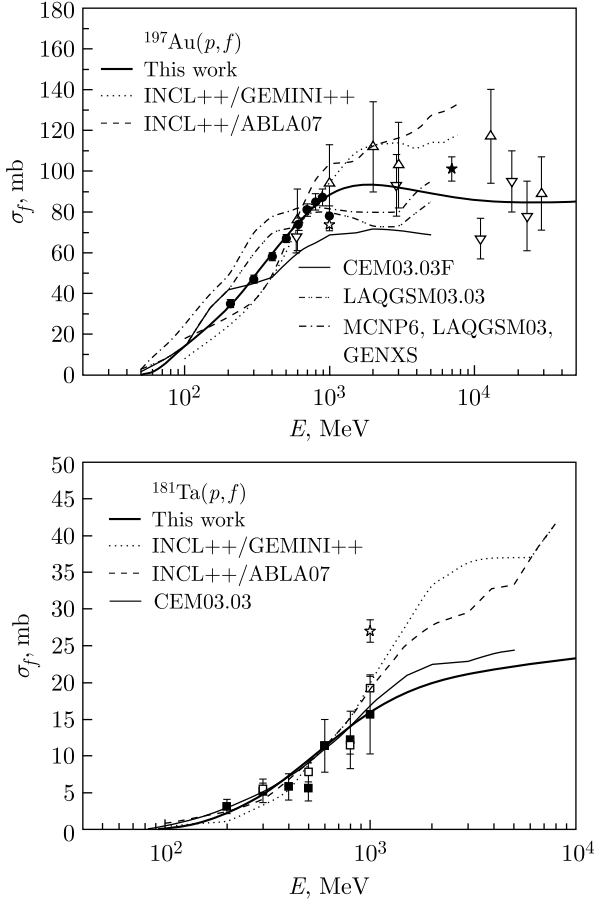
15

Fig. 16. The comparison of the model prediction of the fission cross sections ^{197}Au(p, f) (top) and ^{181}Ta(p, f) (bottom) with the theoretical calculations [10, 12] and experimental data

data is shown in Figs. 15 and 16. For the reaction ^{238}U(p, f) the theoretical results reproduce experimental data well and are close to the model curve in the energy interval from 100 MeV to 8 GeV. However, for pre-actinide nuclei, the results of different theoretical codes have a large scattering and worse prediction potential in comparison with the phenomenological model.

CONCLUSIONS

The novel phenomenological model of fission cross sections in the high-energy region of incident nucleons has been developed on the basis of realistic picture of high-energy nucleon–nucleus interactions. Coming to 1 GeV, two

fast decay processes — spallation and multifragmentation — appear, and as a result, the fission becomes more and more peripheral reaction that leads to a decrease in its probability.

The model reproduces well the most reliable experimental data obtained for various nuclei from Ta to Pu in a wide energy range above 50 MeV. The neutron-induced fission cross sections of ^{235,238}U and ^{209}Bi evaluated in [1, 2] up to 1 GeV and recommended as neutron standards and reference data are reproduced with a deviation less than 5%. This proves validation of the developed model.

At present, different theoretical codes provide results with a rather high discrepancy between each other and with experimental data. Thus, the codes need further improvement, and here the model predictions might be useful as reference data. For proton-induced fission cross sections, the model gives a much better agreement with experimental data than the approximation formula proposed by Prokofiev [13].

The model has high prediction potential for estimation of fission cross section in an area where reliable data are absent. It predicts some main trends for fission cross sections. For actinides, the energy dependence has two wide peaks and falls down with energy above 1 GeV. For pre-actinides, the first peak at about 50 MeV disappears, and the second one degrades with decreasing fissility parameter. In the very high energy region above 10 GeV, the cross sections tend to constant values. The comparison of (n, f) and (p, f) cross sections near the reaction threshold demonstrates that the first reaction has higher cross section for actinides, and the opposite result is observed for pre-actinides. But with an increase in energy above ~ 100 MeV, the ratio of these cross sections becomes close to unity for actinides. For pre-actinides, the discrepancy between (n, f) and (p, f) cross sections becomes small only in the GeV energy range.

Also, it has to be noted that the model has good potential for further improvement of prediction accuracy with the appearance of new results on inelastic and fission cross sections for interactions of high-energy nucleons with heavy nuclei.

REFERENCES

1. *Carlson A. D. et al.* Evaluation of the Neutron Data Standards // Nucl. Data Sheets. 2018. V. 148. P. 143.

2. *Marcinkevicius B., Simalov S., Pronyaev V.* ^{209}Bi(n, f) and ^{nat}Pb(n, f) Cross Sections as a New Reference and Extension of the ^{235}U, ^{238}U and ^{239}Pu(n, f) Standards up to 1 GeV. IAEA, INDC(NDS)-0681. 2015.

3. *Watanabe Y., Kosako K., Kunieda S. et al.* // J. Korean Phys. Soc. 2011. V. 59. P. 1040.

4. *Leya I., Wieler R., David J.-C. et al.* // Nucl. Instrum. Meth. Phys. Res. B. 2005. V. 229. P. 1.

5. *Aydin A., Yalim H. A., Tel E. et al.* // Ann. Nucl. Energy. 2009. V. 36. P. 1307.

6. *Yasin Z.* // Chin. Phys. Lett. 2009. V. 26. P. 082505.

7. *Mancusi D., Charity R. J., Cugnon J.* arXiv:1007.0963v3 [nucl-th]. 14 Sept. 2010.

8. *Maslov V. M.* // J. Korean Phys. Soc. 2010. V. 59. P. 863.

9. *Grudzevich O. T., Yavshits S. G.* // Phys. Atom. Nucl. 2013. V. 76. P. 263.

10. *Mashnik S. G., Sierk A. J., Prael R. E.* arXiv:1303.4308v1 [nucl-th]. 18 Mar. 2013; *Mashnik S. G.* LANL Report LA-UR-15-26166. 2015.

11. *Lo Meo S., Mancusi D., Massimi C. et al.* arXiv:1409.4885v1 [nucl-th] 17 Sept. 2014.

12. *Lo Meo S., Mancusi D., Massimi C. et al.* // Proc. ND2016, EPJ Web Conf. 2017. V. 146. P. 04049.

13. *Prokofiev A. V.* // Nucl. Instrum. Meth. Phys. Res. A. 2001. V. 463. P. 557.

14. *Chestnov Yu. A.* // Phys. Atom. Nucl. 2008. V. 71. P. 2018.

15. *Fukahori T., Kunieda S.* // J. Korean Phys. Soc. 2011. V. 59. P. 975.

16. *Simbel M. H.* // Z. Phys. A: Atom. Nucl. 1989. V. 333. P. 177.

17. *Cugnon J., Volant C., Vuillier S.* // Nucl. Phys. A. 1997. V. 625. P. 729.

18. *Mancusi D., Charity R. J., Cugnon J.* // Phys. Rev. C. 2010. V. 82. P. 044610.

19. *Viola V. E. et al.* // Phys. Rev. Lett. 2004. V. 93. P. 132701.

20. *Turbide S. et al.* // Phys. Rev. C. 2004. V. 70. P. 014608.

21. *Tishchenko V. et al.* // Phys. Rev. Lett. 2005. V. 95. P. 162701.

22. *Budzanowski A. et al.* // Phys. Rev. C. 2008. V. 78. P. 024603.

23. *Porile N. T. et al.* // Phys. Rev. C. 1989. V. 39. P. 1914.

24. *Michel R. et al.* // Nucl. Instrum. Meth. B. 1997. V. 129. P. 153.

25. *Michel R. et al.* // J. Nucl. Sci. Technol., Supp. 2002. V. 2. P. 242.

26. *Ricciardi M. V. et al.* // Phys. Rev. C. 2006. V. 73. P. 014607.

27. *Audouin L. et al.* // Nucl. Phys. A. 2006. V. 768. P. 1.

28. *Balabekyan A. R. et al.* // Phys. Rev. C. 2014. V. 90. P. 054612.

29. *Letaw J. R., Silberberg R., Tsao C. H.* // Astrophys. J. Supp. Ser. 1983. V. 51. P. 271.

30. *Lisowski P. W. et al.* // Neutron Induced Fission Cross Section Ratios for ^{232}Th, ^{235,238}U, ^{237}Np and ^{239}Pu from 1 to 400 MeV // Proc. Int. Conf. on Nuclear Data for Science and Technology, Mito, JAERI, 1988. P. 97.

31. *Paradela C. et al.* // Proc. Int. Conf. on Advances in Nuclear Analysis and Simulations, Vancouver, Canada, 2006. P. B076.

32. *Paradela C. et al.* ^{237}Np(n, f) Cross Section: New Data and Present Status // J. Korean Phys. Soc. 2011. V. 59. P. 1908.

33. *Colonna N.* (n_TOF Collab.). The Fission Experimental Programme at the CERN n_TOF Facility: Status and Perspectives // Eur. Phys. J. A. 2020. V. 56, No. 48. P. 1–49.

34. *Kotov A. A., Vaishnene L. A., Vovchenko V. G. et al.* // Phys. Rev. C. 2006. V. 74. P. 034605.

35. *Vaishnene L. A., Vovchenko V. G., Gavrikov Yu. A. et al.* // Bull. Russ. Acad. Sci.: Phys. 2010. V. 74. P. 496.

36. *Remy G., Ralarosy J., Stein R. et al.* // NucI. Phys. A. 1971. V. 163. P. 583.

37. *Brandt R., Carbonara F., Cieslak E. et al.* // Rev. Phys. Appl. 1972. V. 7. P. 243.

38. *Hudis J., Katcoff S.* // Phys. Rev. C. 1976. V. 13. P. 1961.

39. *Bochagov B. A., Bychenkov V. S., Dmitriev V. D. et al.* // Phys. Atom. Nucl. 1978. V. 28. P. 291.

40. *Khan H. A., Khan N. A.* // Phys. Rev. C. 1984. V. 29. P. 2199.
41. *Yurevich V. I., Nikolaev V. A., Yakovlev R. M., Sosnin A. N.* // Phys. Atom. Nucl. 2002. V. 65. P. 1383.
42. *Schmidt K. H., Jurado B., Pleskač R. et al.* // Phys. Rev. C. 2013. V. 87. P. 034601.
43. *Bernas M., Armbruster P., Benlliure J. et al.* // Nucl. Phys. A. 2003. V. 725. P. 213.
44. *Saint-Laurent F., Conjeaud M., Dayras R. et al.* // Nucl. Phys. A. 1984. V. 422. P. 307.
45. *Konshin V. A., Matusevich E. S., Regushevsky V. I.* // Phys. Atom. Nucl. 1965. V. 2. P. 682.
46. *Shigaev O. E., Bychenkov V. S., Lomanov M. F. et al.* Report RI-17. Leningrad: Radium Institute, 1973.
47. *Rodriguez-Sanchez J. L., Benlliure J., Taïeb J. et al.* // Phys. Rev. C. 2014. V. 90. P. 064606.
48. *Enqvist T. et al.* // Nucl. Phys. A. 2001. V. 686. P. 481.
49. *Yurevich V. I., Nikolaev V. A., Yakovlev R. M., Vorobiev I. B.* // Phys. Part. Nucl. Lett. 2005. V. 2. P. 49.
50. *Tishchenko V., Herbach C.-M., Hilscher D. et al.* // Phys. Rev. Lett. 2005. V. 95. P. 162701.
51. *Ayyad Y., Benlliure J., Casarejos E. et al.* // J. Korean Phys. Soc. 2011. V. 59. P. 1852.
52. *Debeauvais M., Tripier J., Jokic S.* // Proc. 9th Int. Conf. on Solid State Nuclear Track Detectors, 1978, Neuherburg/Munchen. 1978. V. 2 P. 1179.
53. *Debeauvais M., Tripier J., Jokic S., Todorovic Z., Antanasijevic R.* // Phys. Rev. C. 1981. V. 23. P. 1624.

Редактор *Е. И. Кравченко*